Modelling and Forecast of Air Pollution Concentrations during COVID Pandemic Emergency with ARIMA Techniques: the Case Study of Two Italian Cities

D. ROSSI[1], A. MASCOLO[1], S. MANCINI[2], J. G. CERON BRETON[3], R. M. CERON BRETON[3], C. GUARNACCIA[1]

[1]Department of Civil Engineering, University of Salerno, via Giovanni Paolo II 132, 84084, Fisciano, SA, ITALY

[2]Department of Information and Electric Engineering and Applied Mathematics, University of Salerno, via Giovanni Paolo II 132, 84084, Fisciano, SA, ITALY

[3]Chemistry Faculty, Universidad Autónoma del Carmen, Calle 56 n. 4, Col. Benito Juárez, C.P. 24180, Ciudad del Carmen, Campeche, MEXICO

Abstract:- An efficient and punctual monitoring of air pollutants is very useful to evaluate and prevent possible threats to human beings' health. Especially in areas where such pollutants are highly concentrated, an accurate collection of data could suggest mitigation actions to be implemented. Moreover, a well-performed data collection could also permit the forecast of future scenarios, in relation to the seasonality of the phenomenon. With a particular focus on COVID pandemic period, several literature works demonstrated a decreasing of pollutant concentrations in air of urban areas, mainly for NOx, while CO and PM10, on the opposite, has been observed to remain still, mainly because of the intensive usage of heating systems by the people forced to stay home (on specific regions). With the present contribution the authors here present an application of Time Series analysis (TSA) approach to pollutants concentration data of two Italian cities during first lockdown (9 march – 18 may 2020), demonstrating the possibility to predict pollutants concentration over time.

Key-Words: - COVID pandemic, Air pollutant, Environmental monitoring, Time Series modelling, ARIMA

Received: December 19, 2022. Revised: January 31, 2023. Accepted: February 13, 2023. Published: February 24, 2023

1 Introduction

Among all the environmental hazards, air pollutants are the most dangerous, and represent a serious threat to people's health, especially in areas where such pollutants are highly concentrated, [1]. Constantly high levels of pollutants can lead, in fact, to severe cardiovascular and respiratory problems and mortality, both in short-mid then in long term, [2]. To preserve inhabitants' health, it is then mandatory to implement large, effective and prompt monitoring networks to control and register pollutants' concentration over time, [3]. With an accurate data collection it is possible to calibrate and validate models able to predict pollution severity and immediately alert the population, take actions and controls on pollutants sources, and track changes in relation to the seasonality, [4], [5], [6]. A prompt identification of pollutants' concentration is, on the other side, crucial for whatever effective mitigation action to be implemented, [7].

Many scientific works have covered the subject, and lately literature has focused the attention on the COVID pandemic period, [8], [9], observing a general decrease of pollutants in the air of urban areas, mainly for NOx. CO and PM10, on the opposite, have been observed to remain still, mainly because of the intensive usage of heating systems of people forced to stay home (in specific regions). Nevertheless, the mentioned studies offer a deep and yet retrospective statistical analysis of the phenomenon. Other noticeable works present the application of ARIMA models and other deep learning models to implement a pollutant prevision in Bangladesh, [10], and in Turkey, [11].

With the present contribution, the authors propose the results obtained by applying the "Time Series Analysis" (TSA) approach to pollutants concentration data of two Italian cities during the first lockdown (9 March – 18 May 2020), when we observed an unpredictable situation regarding air pollutants.

The aim of this study is twofold: on one hand, to compare the observed concentrations of pollutants with respect to concentrations measured in the same months of 2018 and 2019; on the other hand, to provide a reliable model to forecast the pollutant in urban area by analyzing previously measured concentrations of the same pollutant. The combined effect of the continuous monitoring and the forecast could then provide a secure monitoring network, to profit from the implementation of early decisions regarding the principal pollutants emitters (cars, industries). Collected data have been described in detail, then compared with the values of previous years and finally used to calibrate a predictive model. The TSA approach applied on such datasets is widely documented in literature, [12], [13], [14], [15], assuring the goodness of the adopted methodology. A preliminary analysis of the datasets and the models used in this paper has been published in [16]. In this paper, the complete validation of the models, as well as the forecast and the residuals analysis, will be presented.

2 Material and Methods

Basically, the analysis of a Time Series is the observation and study of the slope of a selected variable over time, in terms of trend and seasonal patterns. Since these techniques can be applied only to continuous datasets, if any problem occurs during the measurements, resulting in a hole in the time series, it’s necessary to impute the missing data. The imputation can be performed in many ways. In particular, the most used are related to regression techniques or modelling imputation, as reported in [17]. Whereas the variable is the only one present, the time series is called *univariate*, and the most used approaches are based on a deterministic decomposition or on Auto-Regressive Integrated Moving-Average (ARIMA) procedures, [18], [19]. The ARIMA(p,d,q) general formula is reported in equation 1:

$$\phi_p(B)(1-B)^d\, Y_t = \theta_q(B)\, e_t \tag{1}$$

where Y_t is the observed variable, B the delay operator, ϕ_p the autoregressive polynomials, θ_q the moving average polynomials, e_t the residual (difference between the observed values and the predicted ones at time t). p, d and q are the model hyperparameters, being respectively the autoregression, differentiation and moving average orders.

In this paper, the calibration and validation of two ARIMA models applied on air pollutants concentrations data is presented. Hyperparameters and coefficient estimation has been performed with “*R*” software, [20], [21], by means of Akaike Information Criterion (AIC) and Bayesian Information Criterion (BIC) criteria optimization. These criteria optimize the balance between likelihood maximization and number of parameters minimization, in order to fulfil the parsimony principle. The AIC and BIC are defined respectively in equations 2 and 3:

$$AIC = -2\ln(L) + 2(k) \tag{2}$$

$$BIC = -2\ln(L) + \ln(n)\cdot(k) \tag{3}$$

where L is the likelihood function, k is the number of estimated parameters in the model and n is the sample size.

3 Case Studies and Dataset Presentation

The case studies presented in this paper are the two Italian cities of Nocera Inferiore and Solofra, both of them in the Campania region (Fig. 1). Data used in the application was obtained from two fixed monitoring stations settled and maintained by ARPAC (*Agenzia Regionale per la Protezione dell’Ambiente Campania*, i.e. Regional Agency for Environmental Protection in Campania) - which is the regional agency taking care of environmental protection. The pictures of external and internal views of the stations are reported in Figure 2.

ARPAC recently announced that the dissemination of air quality data, in the form of daily bulletins, has been resumed on the agency website. The publication of the bulletin, in its traditional form, had been suspended following the hacker attack that hit the Agency's servers in August 2022. However, a periodic summary of the data was published uninterruptedly, and the monitoring stations continued to operate, without any loss of data, even during the months when the daily bulletin was not published.

Fig. 1: Sites location highlighting the Campania region (in red) and the provinces, [16].

Fig. 2: External, [22], and internal, [23], views of the monitoring stations installed by ARPAC.

The two selected monitoring stations continuously record levels of Benzene, NO_2, SO_2, PM_{10}, $PM_{2.5}$ and CO, together with values of humidity and temperature.

The first monitoring station is positioned in Solofra, in the province of Avellino, which is a city having a long history of leather production and tanning, with many industries present and active. As known, leather production and processing, especially tanning processes, involve a massive production of pollutants: Volatile Organic Compounds (VOCs), Particulate Matter (PM), Hydrogen sulphide (H_2S) - responsible for the peculiar bad smell. On the other hand, such industries also engender CO and NO_x, and that's because of the large amount of hot water needed to ensure the tanning procedure. Finally, pollutants coming from industrial sources must be obviously summed to the ones coming from the surrounding sources – private properties, other factories, road traffic.

The monitoring station of Nocera Inferiore is, on the opposite, situated near to a highway and some city roads having high car presence, therefore primarily collecting road traffic pollution levels. In such regard, it is worthy to point out that Nocera Inferiore is one of the most polluted cities of the Campania Region: in 2020, for instance, PM_{10} concentrations exceeded the allowed threshold 67 times over the 35 permitted by law, [24]. The monitoring station is positioned on a residential downtown, also having many houses and buildings in the surroundings.

From both the monitoring stations authors have collected, for the presented analysis, PM_{10} and CO daily concentrations, in a timespan going from February to May 2020.

According to the study on the air quality over the time span 2015-2021, provided by ARPAC in 2022, [25], in Campania region PM_{10} concentrations are mainly due to non-industrial combustion plants that contribute more than 67% in 2016. Transport roads account for about 13% of PM_{10} emissions. The agriculture sector is responsible for more than 9% of emissions and Industrial processes without combustion for about 4%. A non-negligible contribution comes from forest fires, with a 3% share.

As for CO, the same document, [25], reports that the main carbon monoxide emissions in Campania region are from vehicle exhausts, while other emission sources are heating systems and industrial processes. However, the continuous development of the technologies has made it possible to minimise the presence of this pollutant in the air. In 2016, emissions of CO were mainly due to the road transport sector for over 48% and non-industrial combustion plants for about 45%.

At first, the selected datasets for PM_{10} and CO levels have been compared with those measured in the same time span of 2018 and 2019. To visualize the trends, data were organized using a bar plot after aggregating them by month of collection (Fig. 3). A line plot has been subsequently plotted, with aggregation by week (Fig. 4). In detail, the authors highlighted in green the period of public restrictions, going from the 4^{th} of March when public schools were closed and the first phase of lockdown started, up to the 17^{th} of May.

For a better comprehension of the succession of events during the mentioned period, the dates and description of containment measures imposed by law on the Italian population during COVID pandemic burst are reported in Table 1.

In Figures 3 and 4 it can be noticed that, even if during lockdown road traffic drastically decreased, a substantial lowering of pollutant concentration has not been recorded for CO and PM_{10}. The reason is maybe due to the fact that people forced to stay home extensively used heating systems, contributing to a higher level of CO. All the people staying home, in fact, by using boilers, which are often based on old functioning systems, with large emissions and gas consumption, increased the absolute value of pollution sources.

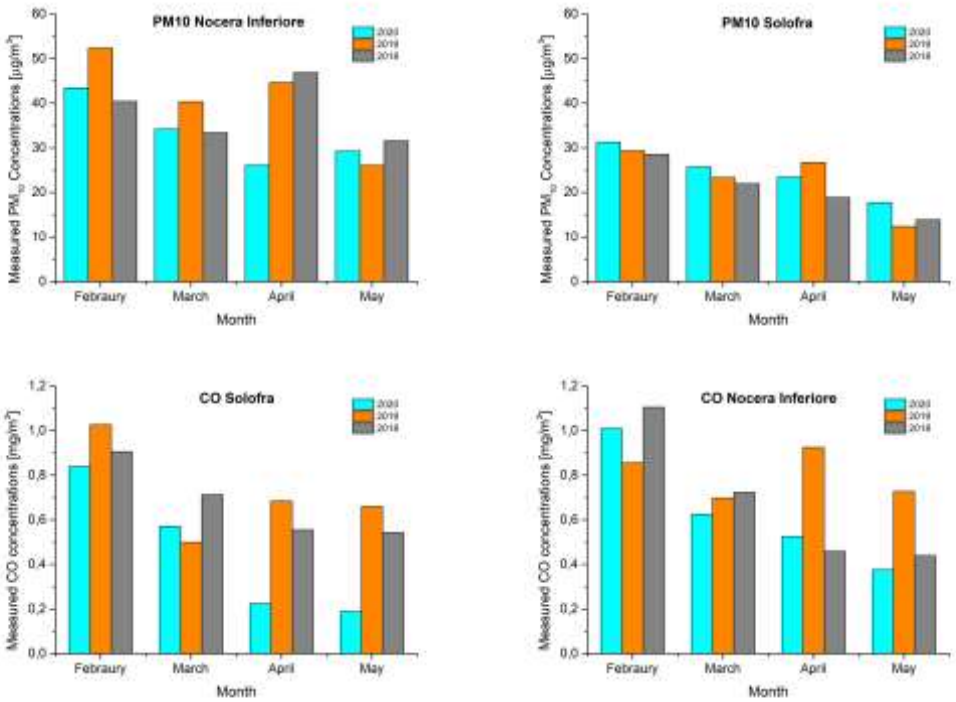

Fig. 3: Average monthly levels of PM_{10} and CO registered in Nocera Inferiore and Solofra from February to May 2018, 2019 and 2020.

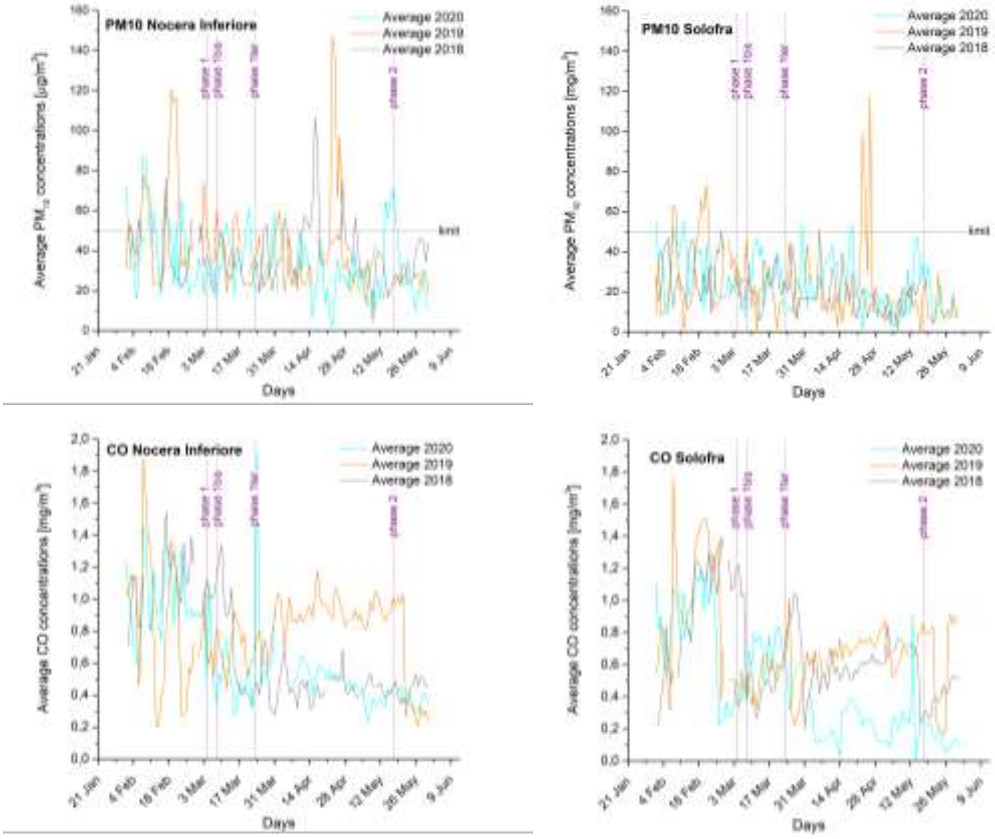

Fig. 4: Average daily levels of PM_{10} and CO registered in Nocera Inferiore and Solofra from February to May 2018, 2019 and 2020 with evidence of the different restriction phases. The red dashed line in PM_{10} plots is the threshold for daily concentration that the Italian regulation allows to overcome 35 days per year.

Table 1. Timeline of the Italian governmental restriction from February to May 2020

Phase	Decree of the Government	Adopted containment measures
1	4th of March 2020	Suspension of all educational activities (all levels schools and universities)
1bis	8th of March 2020	Total lockdown of all the cities
1ter	23rd of March 2020	Closure of all activities excepted essential industrial and commercial ones
2	17th of May 2020	End of restriction on displacement among cities and regions

During the same periods of 2018 and 2019 large part of the population was in working places and schools, which are energetically more efficient, from the pollution point of view, than private residential units. As an example, University of Salerno uses photovoltaic roofs and plants to produce 30% of the energy needed for daily activities of the about 1000 professors and researchers, 500 technicians and administrative staff, plus all the people working in the lab and the 35000 students, [26].

For the aforementioned reasons the authors decided to calibrate and test (validate) the chosen model with the datasets on CO for the city of Solofra and on PM_{10} datasets for Nocera Inferiore.

Two different approaches have been used for imputing missing data: for CO datasets we choose to impute with mean value between precedent and successive values. For PM_{10} we used, instead, the "cold neck" technique, meaning that missing values have been substituted with the values coming from concentrations observed in the same period of previous years. In such a way we were able to preserve the mean and the standard deviation of the whole data distribution, as visible in Tables 2 and 3.

4 Results and Discussion

In this work, the authors implemented three TSA models, which have been tuned and validated in "*R*" software. All the models are based on ARIMA, and they have been calibrated by minimizing AIC and BIC criteria, according to the parsimony principle.

4.1 PM10 Concentrations in Nocera Inferiore

After checking the autocorrelation and partial autocorrelation (Fig. 5), an AR(1) model is suggested for the PM_{10} concentrations in Nocera Inferiore, having only order 1 autoregressive component. Moreover, the routine "*auto.arima*" implemented in the forecast package of "*R*" software, also hinted at such a choice.

Figure 6 shows the existing overlap between PM_{10} values measured and simulated, observing a one-day delay in the prediction.

Figure 7, instead, reports on the left a scatter plot correlating observed and simulated level of PM_{10} concentrations. It is remarkable that 80.2% of the simulations lie in the area determined by average of the observation ± one standard deviation. Especially in the low concentration range, the plot shows a certain number of overestimations in the simulated values of PM_{10}, while in the high concentration range underestimated simulated values are present. On the right side of Figure 7, the histogram of the residuals of the model, i.e. the difference between observed and simulated values, is plotted, while the summary statistics of the distribution of the residuals are reported in Table 4. The obtained kurtosis index is a positive value, which indicates that the distribution is leptokurtic. This is consistent with what can be discerned by observing the histogram: the trend of the residuals has a more "pointed" shape than a normal Gaussian distribution. Furthermore, the positive skewness index is properly substantiated by the evidence that a rightward tail is present in the histogram.

D. Rossi, A. Mascolo, S. Mancini,
J. G. Ceron Breton, R. M. Ceron Breton,
C. Guarnaccia

Table 2. Summary statistics of the CO concentrations measured in Solofra.

Calibration dataset	Mean [mg/m^3]	Std. Dev. [mg/m^3]	Median [mg/m^3]	Skew	Kurt
Observed	0.45	0.32	0.33	0.71	-0.77
Reconstructed	0.45	0.32	0.35	0.72	-0.79

Table 3. Summary statistics of the PM_{10} concentrations measured in Nocera Inferiore.

Calibration dataset	Mean [µg/m^3]	Std. Dev. [µg/m^3]	Median [µg/m^3]	Skew	Kurt
Observed	33.44	17.13	29.75	0.81	0.23
Reconstructed	33.53	17.04	29.50	0.80	0.19

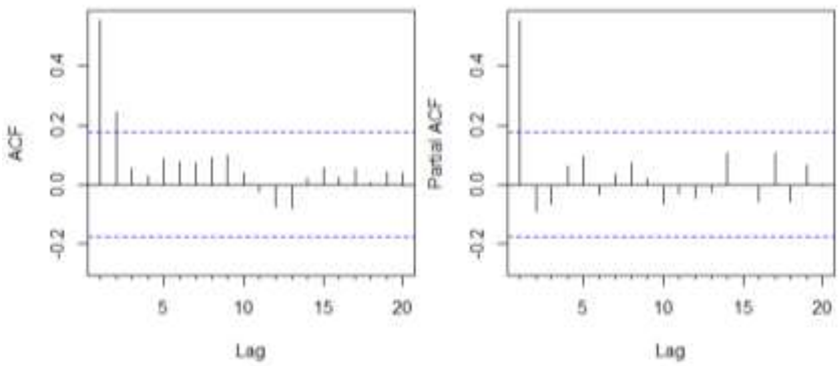

Fig. 5: Autocorrelation and Partial autocorrelation for PM_{10} observed in Nocera Inferiore, [16].

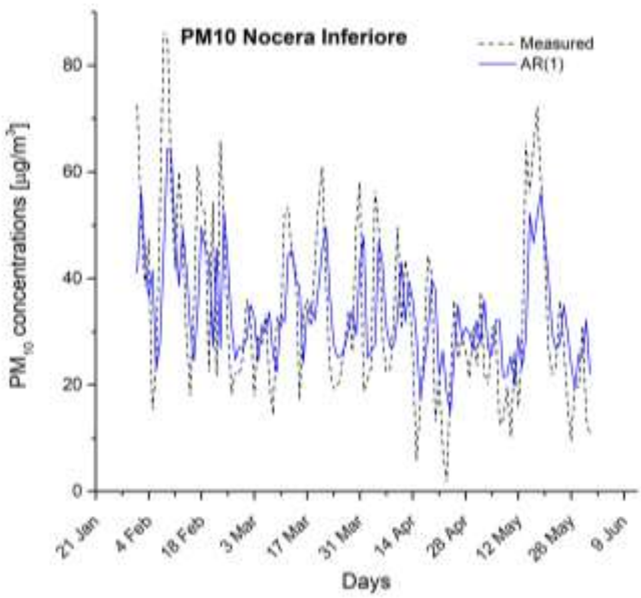

Fig. 6: Plot of observed and simulated PM_{10} concentrations in Nocera Inferiore in the calibration phase.

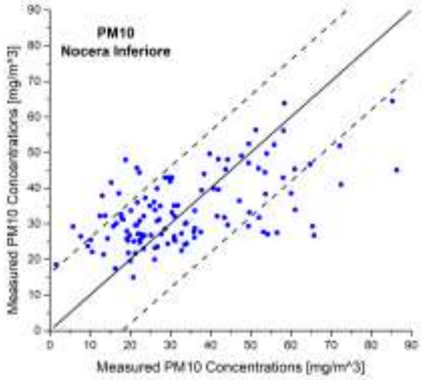

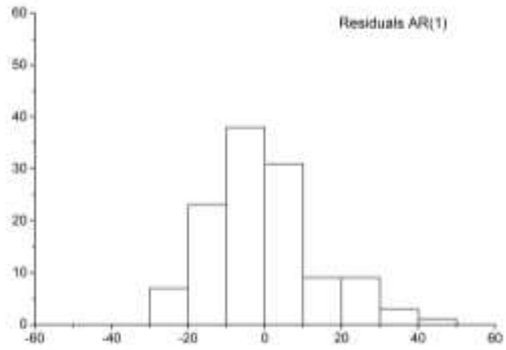

Fig. 7: Scatterplot of observed and simulated PM_{10} concentrations in Nocera Inferiore in the calibration phase and histogram of the residuals.

Table 4. Summary statistics of the residuals of AR(1) model for PM_{10} concentrations - Nocera Inferiore

	Mean [µg/m^3]	Std. Dev. [µg/m^3]	Median [µg/m^3]	Skew	Kurt
Residuals AR(1)	-0.25	13.99	-2.22	0.62	0.36

4.2 CO Concentrations in Solofra

The same analysis implemented for PM_{10} concentration in Nocera Inferiore has been produced by using the data of CO concentration in Solofra, obtaining the same graphs.

The series generated with this dataset is nonstationary, thus a differentiation became necessary in order to work with a smoother time series. By looking at the autocorrelation and the partial autocorrelation plots (Fig. 8) the authors decided to choose a ARIMA(14,1,14) model, which was tested together with the ARIMA(0,1,1) simple model suggested by the BIC criterion (a ranking has been obtained with the "*arimaId*" function of the "*ast*" package in the "*R*" software). Figure 9 shows the slope of the measured CO concentrations overlapped with the two ARIMA models results. Both the models are good enough in fitting CO concentrations curve, but ARIMA(0,0,1) has a certain delay in the process. ARIMA(14,1,14), on the contrary, does not exhibit the delay, but its implementation requires a higher computational effort due to the large number of parameters. In Figure 10 it can be appreciated how the entirety of the simulations obtained both with ARIMA(0,1,1) and ARIMA(14,1,14) have a high level of accuracy, since they are in the region outlined by average of the observation ± one standard deviation.

The summary statistics of the distribution of residuals for both models are reported in Table 5 and their histograms are plotted in Figure 11.

In the ARIMA(0,1,1) model, both the skewness index and the kurtosis index are positive values. Indeed, this model can be described as a leptokurtic-type distribution of residuals, with positive skewness. In the ARIMA(14,1,14) model, on the other hand, the negative skewness index and positive kurtosis index identify a leptokurtic distribution, but with negative skewness.

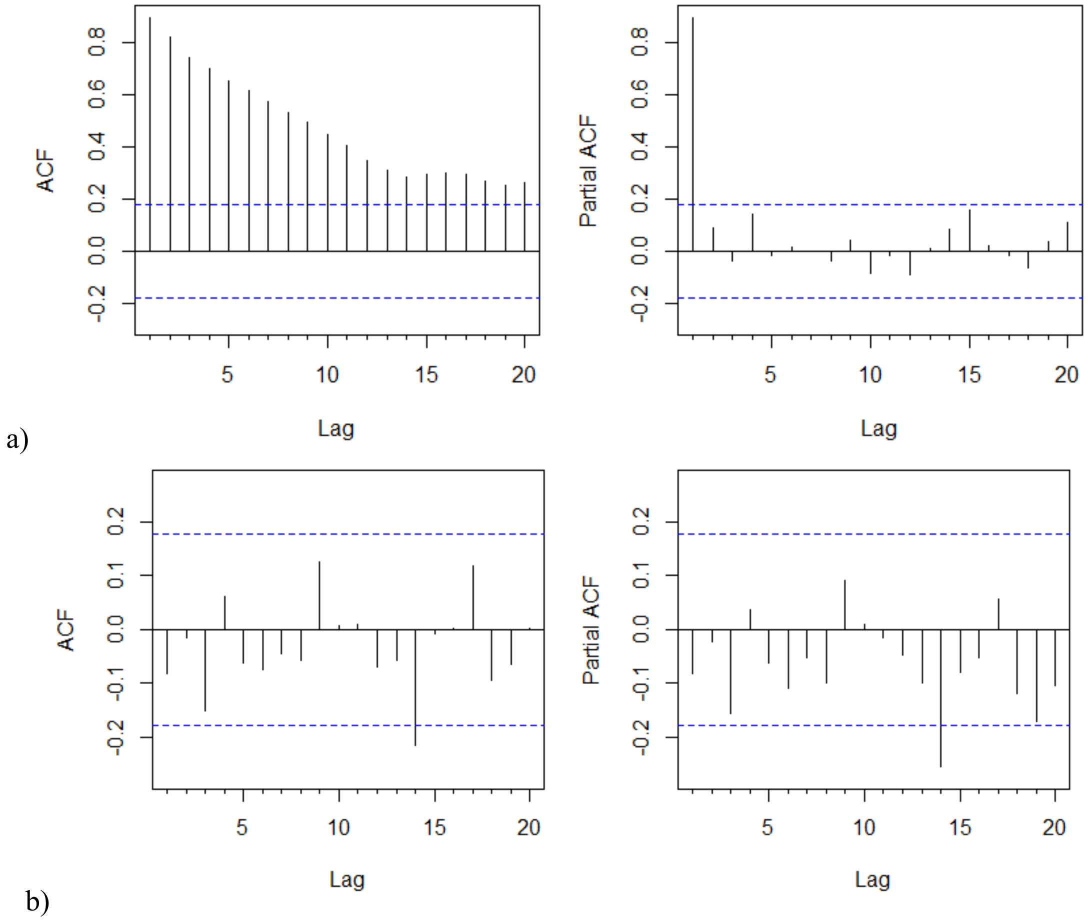

Fig. 8: Autocorrelation and Partial autocorrelation for CO a) observed series and b) differenced series in Solofra, in calibration phase, [16].

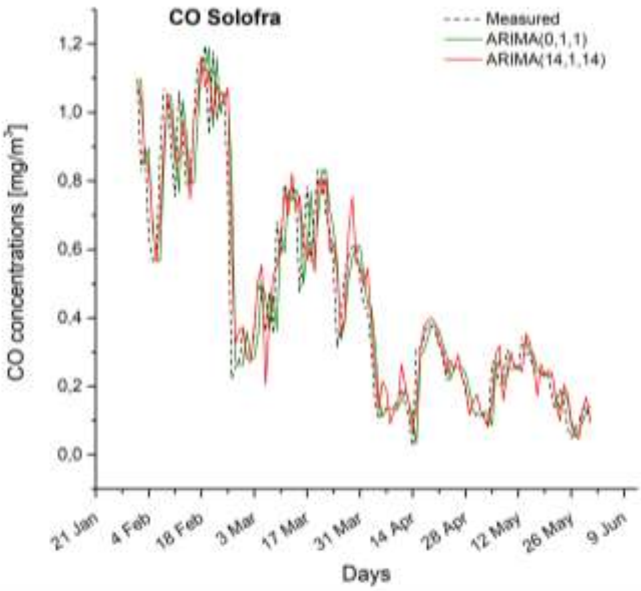

Fig. 9: Plot of observed and simulated CO concentrations in Solofra, with ARIMA(0,1,1) and ARIMA(14,1,14) during the calibration phase.

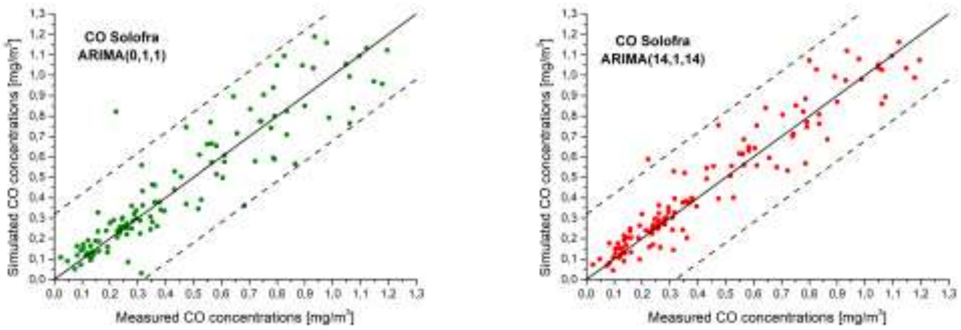

Fig. 10: Scatter plot of observed and simulated CO concentrations in Solofra, during the calibration phase, with ARIMA(0,1,1) on the left, and ARIMA(14,1,14) on the right.

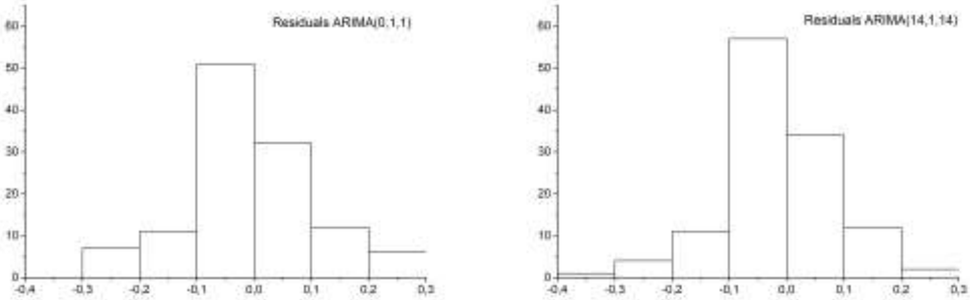

Fig. 11: Histograms of the residuals of the ARIMA(0,1,1) model on the left and the ARIMA(14,1,14) model on the right for CO concentrations – Solofra.

Table 5. Summary statistics of the ARIMA(0,1,1) and ARIMA(14,1,14) models residuals for CO concentrations – Solofra.

	Mean [mg/m^3]	Std. Dev. [mg/m^3]	Median [mg/m^3]	Skew	Kurt
Residuals ARIMA(0,1,1)	-0.01	0.13	-0.01	0.51	3.45
Residuals ARIMA(14,1,14)	-0.02	0.1	-0.02	-0.31	1.56

5 Forecast Results

The ARIMA models can be used to forecast future variations of the analyzed pollutants, to be then compared with actual collected data. By accurately choosing hyperparameters *p*, *d* and *q*, in section 4 different models were found to describe PM_{10} and CO time slope. Thus, hereafter the procedure and results of forecasting on the same pollutants by using the selected models, are reported.

5.1 AR(1) Model Forecast for PM_{10}

The forecast of PM_{10} values in Nocera Inferiore has been generated for the 10 days after the last day used for calibration (31st of May). This interval has been selected since it ensures a quite large time range for possible mitigation actions. The forecasts, in fact, can be used to support policy makers and local governments in the decision process, allowing to prevent large numbers of exceedances of the safe thresholds. In Figure 12 a forecast plot is represented, showing PM_{10} concentration as a function of "future" days.

The forecasted values strictly lie above the measurements, indicating a general overestimation of the model. This is confirmed by the statistical values of the errors reported in Table 6. Even if this slight overestimation could be interpreted as a limitation of the model, in a practical application, overestimating a pollutant is a safe approach, since the possible mitigation actions driven by such forecasts would follow a precautionary principle.

5.2 ARIMA Models Forecasting for CO

Data of CO values recorded in Solofra have also been forecasted for the first ten days after 31st of May 2020, i.e. the days immediately subsequent to the removal of lockdown restrictions. Again, the forecast interval has been chosen to provide useful

D. Rossi, A. Mascolo, S. Mancini,
J. G. Ceron Breton, R. M. Ceron Breton,
C. Guarnaccia

information on the pollutant concentration slope over time. A 10 days' time range is large enough to observe the increasing or decreasing trend in the data and to decide if any intervention is needed.

Results of both ARIMA(0,1,1) and ARIMA (14,1,14) are reported respectively in Figure 13. In this case the predicted values provided by both models exhibit a general underestimation, even though the increasing trend is detected by the ARIMA(14,1,14). The error summary statistics are reported in Table 7.

The good agreement shown by both the models at the very first periods (2 days) suggests that these models can be used to provide useful information for the decision process of the policy makers in a short time range. The continuous measurements collected by the monitoring stations allow to recalibrate the models day by day, making it possible to test the daily forecast and to move further the predictions.

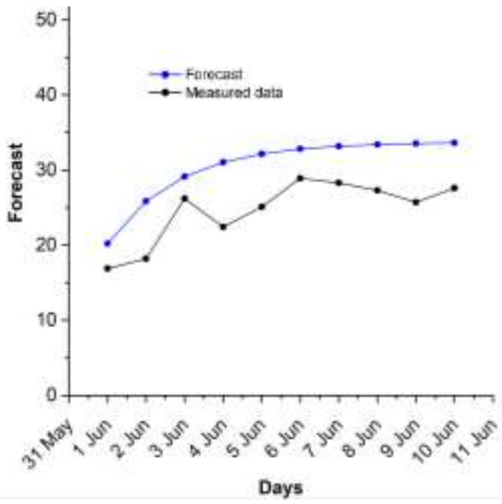

Fig. 12: Plot of observed and forecasted PM_{10} concentrations in Nocera Inferiore.

Table 6. Summary statistics of the errors of AR(1) model for PM10 concentrations - Nocera Inferiore.

Errors	Mean [μg/m³]	Std. Dev. [μg/m³]	Median [μg/m³]
AR(1)	5.83	2.00	6.06

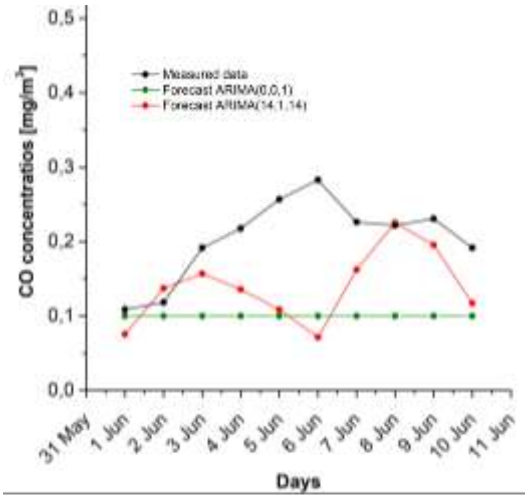

Fig. 13: Plot of observed and simulated CO concentrations in Solofra in the forecast phase, for ARIMA(0,1,1) model (green line) and ARIMA(14,1,14) model (red line).

Table 7. Summary statistics of the errors of ARIMA(0,1,1) and ARIMA(14,1,14) models for CO concentrations - Solofra.

Errors	Mean [mg/m³]	Std. Dev. [mg/m³]	Median [mg/m³]
ARIMA(0,1,1)	0.07	0.07	0.05
ARIMA(14,1,14)	-0.10	0.06	0.12

6 Conclusions

Italy has been hardly affected by COVID-19 explosion, and was one of the first nations to implement a drastic containment policy to limit virus spread and contagion. Trying to mitigate the pandemic, in fact, many governmental restrictions were adopted starting from February 2020.

By analysing the outcomes of such restrictions, the presented work investigated the variations of CO and PM_{10} levels in the Campania region and how ARIMA models could perform good simulation of data. In order to compare how governmental restrictions altered such pollutants' concentrations, two selected cities of the region were chosen. The first is Solofra, in the province of Avellino, an industrial city where leather tanning processing daily takes place. The second one is Nocera Inferiore, in the province of Salerno, which has a high population density (about 2200 inhabitants/km²) and a widespread and busy road network (also a highway barrier). By choosing the two presented cities the authors wanted to evaluate how the pandemic affected two main sources of pollution: the industrial activities and the road traffic together with the population activities

(Nocera Inferiore is also characterized by the close presence of residential areas, schools, shops, highways and small industries).

To evaluate the pollution variations in the considered areas, data recorded from two environmental monitoring stations have been used, and data of the February-May period over three different years have been compared: 2018, 2019, 2020. By using proper physic-mathematical models, the variation of the temporal trend of pollutants before (2018, 2019) and during COVID-19 lockdown (2020) has been assessed through the calibration and validation of models on interesting selected series: CO for Solofra and PM_{10} for Nocera Inferiore. ARIMA models applied showed good performance in the simulation of data. As a result, the authors observed how restriction policies did not significantly contribute to reducing PM_{10} and CO concentrations in air, also compared to previous years. ARIMA models also permit to implement a prediction of the pollutants levels over time, and the authors specifically performed a 10-days forecast of both PM_{10} and CO concentrations, respectively in Nocera Inferiore and Solofra. ARIMA models selected for the forecasting gave results approximately good in a very short prediction range, as documented in literature.

The main limitation of this study relies on the fact that going further from the start of the forecast period, the simulated concentrations start to be significantly different from the observed values. This means that a possible improvement can be the automatic recalibration of the model, day by day, taking into account the latest measurements of the pollutants under study and their possible slope variations. In future works, a parameter sensitivity analysis could be performed to achieve an estimation of the maximum range of prediction that can be used before the need to recalibrate the model. Once the optimal time range is set, the recalibration procedure will provide a reliable predictive model, constantly updated, that could help decision makers in implementing temporary or permanent actions to mitigate the pollutants concentrations, to fulfil the thresholds imposed by the national regulations and to protect human beings' health.

References:

[1] Thieriot H., Myllyvirta L., *Air pollution returns to European capitals: Paris faces largest rebound*, Centre for Research on Energy and Clean Air (CREA), 2020.

[2] Brunekreef B., Holgate S. T., Air pollution and health, *Lancet*, Vol. 360(9341), 2002, pp. 1233-1242.

[3] Cabaneros S, Calautit J K, Hughes B R, A review of artificial neural network models for ambient air pollution prediction. *Environmental Modelling & Software*, Vol. 119, 2019, pp. 285-304.

[4] Achcar J. A., Rodrigues E. R., Guadalupe T., Using non-homogeneous Poisson models with multiple change-points to estimate the number of ozone exceedances in Mexico City, *Environmetrics*, Vol. 22, N. 1, 2011, pp.1-12

[5] Guarnaccia C, Lenza TLL, Mastorakis NE and Quartieri J, A comparison between traffic noise experimental data and predictive models results, *International Journal of Mechanics*, Vol. 5 (4), 2011, pp. 379-386

[6] Liao K, Huang X, Dang H, Ren Y, Zuo S, Duan C, Statistical Approaches for Forecasting Primary Air Pollutants: A Review. *Atmosphere*, Vol. 12, 2021, 686.

[7] Cerón Bretón J. G., Cerón Bretón R.M., Morales S.M., Kahl J.D.W., Guarnaccia C., del Carmen Lara Severino R., Marrón M.R., Lara E.R., de la Luz Espinosa Fuentes M., Chi M.P.U., Sánchez G.L., Health risk assessment of the levels of BTEX in ambient air of one urban site located in Leon, Guanajuato, Mexico during two climatic seasons, *Atmosphere*, Vol. 11, N. 21, 2020.

[8] Rovetta A. The Impact of COVID-19 Lockdowns on Particulate Matter Emissions in Lombardy and Italian Citizens' Consumption Habits. *Frontiers in Sustainability,* Vol. 2, 2021, 649715.

[9] Bray CD, Nahas A, Battye WH, Aneja VP. Impact of lockdown during the COVID-19 outbreak on multi-scale air quality. 2021, *Atmospheric Environment*, Vol. 254, 1994, 118386.

[10] Shahriar S., Kayes I., Hasan K., Hasan M., Islam R., Awang N.R., Hamzah Z., Eh Rak A., Salam M.A., Potential of ARIMA-ANN, ARIMA-SVM, DT and CatBoost for Atmospheric PM2.5 Forecasting in Bangladesh, *Atmosphere* Vol. 12, 1, 2021, 100.

[11] Aladağ E., Forecasting of particulate matter with a hybrid ARIMA model based on wavelet transformation and seasonal adjustment, *Urban Climate* Vol. 39, 2021, 100930.

[12] Guarnaccia C, Quartieri J, Tepedino C., *Deterministic decomposition and seasonal ARIMA time series models applied to airport noise forecasting*, Proc. of the Int. Conf. on Applied Mathematics and Computer Science, AIP Conference Proceedings 1836, 2017, pp. 1-7.

[13] Guarnaccia C, Quartieri J, Mastorakis NE and Tepedino C, Development and application of a time series predictive model to Acoustical noise levels *WSEAS Transactions on Systems,* Vol. 13, 2014, pp. 745-756.

[14] Guarnaccia C, Quartieri J, Rodrigues ER and Tepedino C, Acoustical noise analysis and prediction by means of multiple seasonality time series model, *International Journal of Mathematical Models and Methods in Applied Sciences, Vol.* 8, 2014, 384-393

[15] Guarnaccia C, Cerón Bretón J G, Quartieri J, Tepedino C, Cerón Bretón C R., An Application of Time Series Analysis for Forecasting and Control of Carbon Monoxide Concentrations, *International Journal of Mathematical Models and Methods in Applied Sciences,* Vol. 8, 2014, pp 505-515.

[16] Mancini S., Francavilla A.B., Graziuso G., Guarnaccia C, *An Application of ARIMA modelling to air pollution concentrations during covid pandemic in Italy*, Journal of Physics: Conference Series, Vol. 2162**,** 2022, 012009.

[17] Guarnaccia C., Quartieri J., Tepedino C., Petrovic L., A Comparison of Imputation Techniques in Acoustic Level Datasets, *International Journal of Mechanics*, Vol. 9, 2015, pp. 272-278.

[18] Guarnaccia C., Ceron Breton J. G., Ceron Breton R. M., Tepedino C., Quartieri J., Mastorakis N. E., *ARIMA models application to air pollution data in Monterrey, Mexico*, in AIP Conference Proceedings Vol. 1982, No. 1, 2018, p. 020041.

[19] Guarnaccia C, Mancini S, Quartieri J, Ceron Breton JG, Ceron Breton RM, Prediction of CO Concentrations in Monterrey, Mexico, by means of ARIMA Models, *WSEAS Transactions on Environment and Development*, Vol. 14, 2018, pp. 653-661.

[20] Cryer P D, Chan K. Time Series Analysis, with applications in R. 2008.Second Edition, Springer.

[21] R Core Team (2018). R: A language and environment for statistical computing. R Foundation for Statistical Computing, Vienna, Austria.

[22] ARPA Campania*, Qualità dell'aria in Campania: monitoraggio mai interrotto, riprende pubblicazione bollettini*, available online: https://www.arpacampania.it/-/qualit%C3%A0-dell-aria-in-campania-monitoraggio-mai-interrotto-riprende-pubblicazione-bollettini, in Italian, last accessed on February 10, 2023.

[23] ARPA Campania*, Qualità dell'aria: dati orari su polveri sottili in altre 20 stazioni di monitoraggio in Campania*, available online: https://www.arpacampania.it/-/qualita-dell-aria-dati-orari-su-polveri-sottili-in-altre-20-stazioni-di-monitoraggio-in-campania, in Italian, last accessed on February 10, 2023.

[24] Gazzetta Ufficiale della Repubblica Italiana (2010). Ministerial Decree August 13, 2010 n.155. Available online at: https://www.camera.it/parlam/leggi/deleghe/testi/10155dl.html .

[25] ARPAC (2022), *La qualità dell'aria in Campania*, 2015-2021, available online: https://www.arpacampania.it/web/guest/relazioni-e-report, last accessed on February 10, 2023.

[26] University of Salerno, *Photovoltaic Park of the Campus of Fisciano*, available online: https://web.unisa.it/en/campus-life/campus/photovoltaic-park, last accessed on February 10, 2023.

Contribution of Individual Authors to the Creation of a Scientific Article (Ghostwriting Policy)

Conceptualization: C. Guarnaccia, J.G. Ceron Breton, R.M. Ceron Breton
Data curation: D. Rossi, A. Mascolo, C. Guarnaccia
Methodology: D. Rossi, C. Guarnaccia, J.G. Ceron Breton, R.M. Ceron Breton
Software: D. Rossi, A. Mascolo, C. Guarnaccia
Supervision: C. Guarnaccia
Visualization: D. Rossi, A. Mascolo
Writing - original draft: D. Rossi
Writing - review & editing: all the co-authors
Corresponding authors: D. Rossi, C. Guarnaccia

Sources of Funding for Research Presented in a Scientific Article or Scientific Article Itself

No funding was received for conducting this study.

Conflict of Interest

The authors have no conflicts of interest to declare that are relevant to the content of this article.